Separation Science and Technology
Publication details, including instructions for authors and subscription information:
http://www.informaworld.com/smpp/title~content=t713708471

Electrical Aspects of Adsorbing Colloid Flotation. Y. Nonideal Flocs and Salts

David J. Wilson[a]
[a] Department of Chemistry, Vanderbilt University, Nashville, Tennessee

To cite this Article Wilson, David J.(1976) 'Electrical Aspects of Adsorbing Colloid Flotation. Y. Nonideal Flocs and Salts', Separation Science and Technology, 11: 4, 391 — 409

To link to this Article: DOI: 10.1080/01496397608085331

URL: http://dx.doi.org/10.1080/01496397608085331

SEPARATION SCIENCE, 11(4), pp. 391–409, 1976

Electrical Aspects of Adsorbing Colloid Flotation. V. Nonideal Flocs and Salts

DAVID J. WILSON

DEPARTMENT OF CHEMISTRY
VANDERBILT UNIVERSITY
NASHVILLE, TENNESSEE 37235

Abstract

Three methods are developed for the calculation of adsorption isotherms in precipitate and adsorbing colloid flotation. The Gouy-Chapman model is used in all three, with corrections for the effective volumes of the ions in the ionic atmosphere and of the floc particles. The theories all predict a weak dependence of adsorption isotherm on temperature and a stronger dependence on ionic strength; increasing either variable decreases the surface adsorption. The effects of film surface potential, floc zeta potential, ion and floc effective volumes, and floc-floc screening are examined.

INTRODUCTION

A variety of foam flotation techniques has shown promise in the removal of trace heavy metals and other toxic materials from water; these are discussed in the first five references (*1–5*). We have found adsorbing colloid flotation to be particularly effective, and have utilized it for the removal of a number of heavy metals and fluoride (*5–8*). The technique depends upon electrical interaction between the ionic surfactant film and the charged particles of floc being removed; the magnitude of the attraction markedly decreases as the ionic strength of the aqueous phase is increased, as was noted by Sheiham and Pinfold (*9*). We have used the Gouy-Chapman model of the electric double-layer previously to calculate kinetic effects and equilibrium isotherms for precipitate flotation (*10–13*). Useful references for this approach are the books by Verwey and Overbeek and by Devereux and deBruyn (*14*, *15*), and the method has been used by Jorné and Rubin to explain the effects of ionic size and charge on selectivity in foam fractionation (*16*).

We here extend our earlier calculation of adsorption isotherms to take into account both the finite volume of the floc particles and the finite volume of the salt ions responsible for the ionic atmospheres of the charged surfaces.

FIRST METHOD

We follow Macdonald and Brachman (*17*), taking as our starting point for the calculation of the electric potential in the vicinity of the planar double-layer Eqs. (1)–(4):

$$\frac{\partial c^+}{\partial t} = \frac{1}{6\pi\eta r_+}\frac{\partial}{\partial x}\left(c^+ \frac{\partial \mu^+}{\partial x}\right) = 0 \tag{1}$$

$$\frac{\partial c^-}{\partial t} = \frac{1}{6\pi\eta r_-}\frac{\partial}{\partial x}\left(c^- \frac{\partial \mu^-}{\partial x}\right) = 0 \tag{2}$$

$$\frac{\partial^2 \psi}{\partial x^2} = \frac{-4\pi}{D}\rho \tag{3}$$

$$\rho = e(c^+ - c^-) \tag{4}$$

where $c^{+(-)}$ = cation (anion) concentration, particles/cm^3
$\mu^{+(-)}$ = chemical potential of cations (anions)
$r_{+(-)}$ = effective ionic radius of cations (anions)
η = viscosity
x = distance into the solution from the surface
ψ = electric potential, chosen such that $\psi(x) \to 0$ as x becomes large
D = dielectric constant of the solution
ρ = charge density

At equilibrium Eqs. (1) and (2) yield the result that the $\mu^\pm$ are independent of x. We further assume that we are dealing with a 1–1 electrolyte, the ions of which are of comparable effective radius. We wish to take the finite volume of these ions into account in calculating the electric potential; we do this by choosing an activity coefficient suggested by our earlier work on the effect of the finite volume of floc particles within the framework of a cell model (*12*, *13*). The chemical potentials of the ions are then given by

$$\mu^{\pm}(x) = \mu_0^{\pm} \pm e\psi(x) + kT\log c^{\pm}(x) + kT\log\frac{c_{\max}}{c_{\max} - (c^+ + c^-)} \tag{5}$$

Note that $c_{\max}/[c_{\max} - (c^+ + c^-)]$, the activity coefficient, approaches unity at very low salt concentrations and becomes extremely large as $(c^+ + c^-)$ approaches $c_{\max}$, which is certainly the desired behavior. At large distances from the surface we have

$$\mu^{\pm}(\infty) = \mu_0^{\pm} + kT\log c_\infty + kT\log\frac{c_{\max}}{c_{\max} - 2c_\infty} \tag{6}$$

Since the chemical potentials are independent of x, this yields

$$\log c_\infty + \log\frac{c_{\max}}{c_{\max} - 2c_\infty} = \pm\frac{e\psi(x)}{kT} + \log c^{\pm}(x) + \log\frac{c_{\max}}{c_{\max} - [c^+(x) + c^-(x)]} \tag{7}$$

From Eq. (7) we obtain

$$f^{\pm} = \frac{c^{\pm}}{c_{\max} - (c^+ + c^-)} = \frac{c_\infty}{c_{\max} - 2c_\infty}\exp\left(\pm\frac{e\psi(x)}{kT}\right) \tag{8}$$

from which it can be readily shown that

$$c^{\pm}(x) = \frac{c_{\max}f^{\pm}}{1 + f^+ + f^-} \tag{9}$$

Substitution of Eqs. (8) and (9) into (4), and (4) into (3) then yields a modified Poisson-Boltzmann equation,

$$\frac{d^2\psi}{dx^2} = \frac{A\sinh(e\psi/kT)}{1 + B\cosh(e\psi/kT)} \tag{10}$$

where

$$A = \frac{8\pi e c_\infty}{(1 - 2c_\infty/c_{\max})D}$$

and

$$B = 2c_\infty/(c_{\max} - 2c_\infty)$$

Use of Newton's method then yields a first integral of Eq. (10);

$$\frac{d\psi}{dx} = \frac{-|\psi_0|}{\psi_0}\left[\frac{2AkT}{eB}\log\frac{1 + B\cosh e\psi/kT}{1 + B}\right]^{1/2} \tag{11}$$

Here $\psi_0 = \psi(x = 0)$.

We now examine the distribution of floc particles in the vicinity of the surface. From our earlier work on a cell model (*12*, *13*), a suitable choice for the chemical potential of a floc particle is

$$\mu(x) = \mu_0 + q\psi(x) + kT\log\left[\frac{c'_{\max}}{c'_{\max} - c'}c'\right] \tag{12}$$

where q = charge of floc particle
c' = floc concentration, particles/cm^3
$c'_{\max}$ = maximum possible floc concentration

At equilibrium we have $\mu(x)$ independent of x, which readily yields

$$\frac{c'_\infty}{1 - c'_\infty/c'_{\max}}\exp\left[\frac{-q\psi(x)}{kT}\right] = \frac{c'(x)}{1 - c'(x)/c'_{\max}} \tag{13}$$

from which we obtain

$$c'(x) = \frac{c'_\infty \exp(-q\psi/kT)}{1 + \dfrac{c'_\infty}{c'_{\max}}[\exp(-q\psi/kT) - 1]} \tag{14}$$

We define the surface excess of floc per cm^2, s, as

$$s = \int_0^\infty [c'(x) - c'_\infty]\,dx \tag{15}$$

It is advantageous here to change the variable of integration from x to ψ; when this is done and Eqs. (11) and (14) are substituted into Eq. (15), we obtain

$$s = c'_\infty\left(1 - \frac{c'_\infty}{c'_{\max}}\right)\frac{|\psi_0|}{\psi_0}\left(\frac{eB}{2AkT}\right)^{1/2} \times \int_0^{\psi_0}\frac{[\exp(-q\psi/kT - 1]\,d\psi}{\left\{1 + \dfrac{c'_\infty}{c'_{\max}}[\exp(-q\psi/kT) - 1]\right\}\left\{\log\dfrac{1 + B\cosh(e\psi/kT)}{1 + B}\right\}^{1/2}} \tag{16}$$

The isotherms calculated from Eq. (16) are illustrated in Fig. 1 and 2. The effect of varying c'_{max}, the maximum possible floc concentration, is shown in Fig. 1. We expect c'_{max} to be inversely proportional to the average volume of a floc particle, so that one should multiply s by the molar volume of the floc particles to obtain the volume of floc adsorbed on the surface. (The concentrations in the figures are given in moles per cm^2 or cm^3, rather than molecules per cm^2 or cm^3.) The effect of the maximum possible salt concentration, c_{max}, is shown in Fig. 2. Decreasing c_{max} results in a thicker, more diffuse ionic atmosphere, which in turn permits the adsorption of more floc particles. We hope to test this result experimentally by floc flotation of ferric hydroxide from solutions in which salts of markedly different ionic radii are used to adjust the ionic strength. In view of the results shown, we do not anticipate that the effect will be a large one; c_{max} for $CsClO_4$ is expected to be of the order of 0.014 mole/cm^3, assuming no hydration. If a hydration sphere is taken into account, this figure might be reduced to roughly 10^{-3} mole/cm^3.

At high floc concentrations the isotherms are seen to go through maxima, as shown in Fig. 3 for two different ionic strengths, and in Fig. 4 for various temperatures. The adsorption isotherms are seen to depend on temperature only weakly, as we have observed qualitatively in our experimental work.

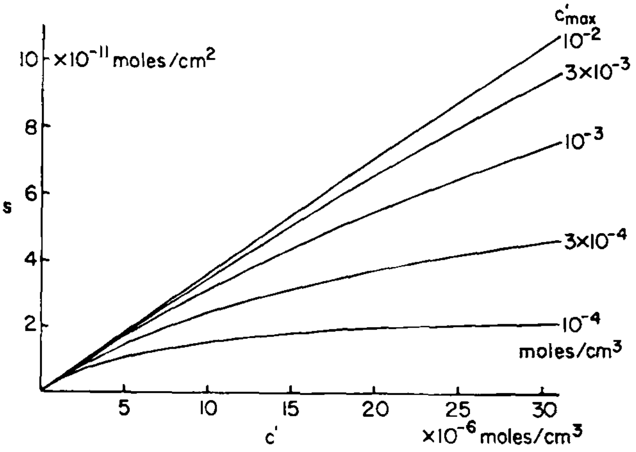

FIG. 1. First method. Plot of surface excess of floc (s) versus floc concentration (c'); effect of c'_{max}. $\psi_0 = -100$ mv, $T = 298\,°K$, $q = 1|e|$, $c_\infty = 10^{-5}$ mole/cm^3, $c_{max} = 10^{-2}$ mole/cm^3.

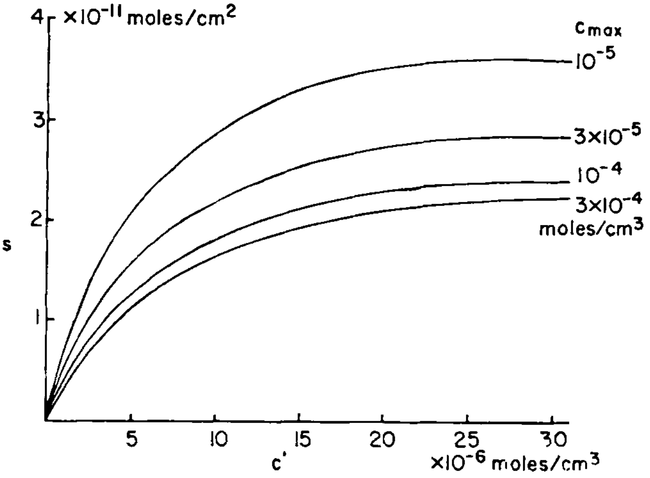

FIG. 2. Plot of s versus c'; effect of varying $c_{\max}$. $\psi_0 = -100$ mv, $T = 298\,^\circ$K, $c_\infty = 10^{-5}$ mole/cm³, $q = 1|e|$.

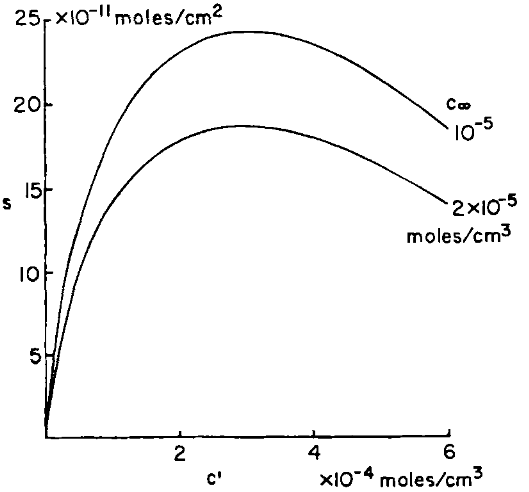

FIG. 3. Plot of s versus c'; effect of varying c_∞. $\psi_0 = -100$ mv, $T = 298\,^\circ$K, $c_{\max} = 10^{-4}$ mole/cm³, $c'_{\max} = 10^{-3}$ mole/cm³, $q = 1|e|$.

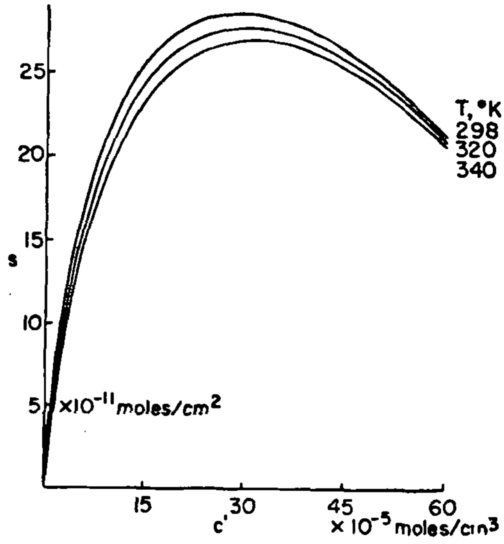

FIG. 4. Plot of s versus c'; effect of temperature. $\psi_0 = -100$ mv, $c_\infty = 10^{-5}$, $c_{\max} = 3 \times 10^{-5}$, $c'_{\max} = 10^{-3}$ mole/cm^3, $q = 1|e|$.

SECOND METHOD

Our first approach, outlined above, provides us with a very rapid, cheap way of computing adsorption isotherms with inclusion of nonideal effects; it does not permit us, however, to take into account the formation of an ionic atmosphere in the vicinity of the floc surface. To include this in our consideration, we modify a method used by Devereux and deBruyn (*15*).

Let the potential of the surfactant-coated surface be ψ_0, the surface potential of the floc particle be ψ_1, and the distance between the surfactant film and the surface presented toward it by the floc particle be l. Let the surface area presented toward the film by the floc particle be a^2. Our modified Poisson-Boltzmann equation is Eq. (10), with boundary conditions $\psi(0) = \psi_0$, $\psi(l) = \psi_1$. Integration of Eq. (10) twice then leads to the result

$$x(\psi) = \int_{\psi_0}^{\psi} \frac{-(|\psi_0|/\psi_0)\,d\psi'}{\left\{\left[\dfrac{d\psi(0)}{dx}\right]^2 + \dfrac{2AkT}{eB}\log\dfrac{1 + B\cosh e\psi'/kT}{1 + B\cosh e\psi_0/kT}\right\}^{1/2}} \qquad (17)$$

We calculate $d\psi(0)/dx$ from the requirement that

$$l = \int_{\psi_0}^{\psi_1} \frac{-(|\psi_0|/\psi_0)\, d\psi'}{\left\{\left[\dfrac{d\psi(0)}{dx}\right]^2 + \dfrac{2AkT}{eB}\log\dfrac{1 + B\cosh e\psi'/kT}{1 + B\cosh e\psi_0/kT}\right\}^{1/2}} \tag{18}$$

We define

$$H(l) = (d\psi(0)/dx)^2 \tag{19}$$

Now the electric force of attraction per unit area of floc presented is given by $\frac{1}{2}D(d\psi/dx)^2$. The osmotic force of repulsion per unit area is zero in that plane where $\psi(x) = 0$. So the force per floc particle presenting area a^2 to the surface is given by

$$f = \frac{a^2D}{2}\left(\frac{d\psi}{dx}\right)^2\bigg|_{\psi=0} \tag{20}$$

Now the first integral of Eq. (10) yields

$$\left(\frac{d\psi}{dx}\right)^2 = H(l) + \frac{2AkT}{eB}\log\frac{1 + B\cosh e\psi/kT}{1 + B\cosh e\psi_0/kT} \tag{21}$$

so that at $\psi = 0$ we have

$$\left(\frac{d\psi}{dx}\right)^2\bigg|_{\psi=0} = H(l) - \frac{2AkT}{eB}\log\frac{1 + B\cosh e\psi_0/kT}{1 + B} \tag{22}$$

Then the electrical contribution to the free energy of the floc particle is given by

$$\begin{aligned} G_{\text{elec}}(l) &= -\int_l^\infty f(l')\, dl' \\ &= -\frac{a^2D}{2}\int_l^\infty \left(\frac{d\psi}{dx}\right)^2\bigg|_{\psi=0} dl' \\ &= \frac{-a^2D}{2}\int_l^\infty \left[H(l') - \frac{2AkT}{eB}\log\frac{1 + B\cosh e\psi_0/kT}{1 + B}\right] dl' \end{aligned} \tag{23}$$

We then obtain an expression for the local floc concentration by replacing $q\psi(x)$ in Eq. (14) by $G_{\text{elec}}(x)$. The surface excess of floc is defined as before, and we obtain finally

$$s_{\text{excess}} = c'_{\infty}\left(1 - \frac{c'_{\infty}}{c'_{\text{max}}}\right)\int_0^{\infty} \frac{1 - \exp\left[G_{\text{elec}}(x)/kT\right]}{\left(1 - \frac{c'_{\infty}}{c'_{\text{max}}}\right)\exp\left[G_{\text{elec}}(x)/kT + \frac{c'_{\infty}}{c'_{\text{max}}}\right.} dx \tag{24}$$

Unfortunately, the numerical evaluation of Eq. (24) via the use of Eq. (23) consumes an excessive amount of machine time. We therefore employ an alternate approach (*15*), using as our starting point

$$G(l) = -\frac{Da^2}{8\pi l}(\psi_1 - \psi_0)^2 + a^2\int_0^1\int_0^l \frac{\rho^1\psi^1}{\lambda}\,dx\,d\lambda \tag{25}$$

Now

$$\rho^1 = -\frac{D}{4\pi}\frac{\partial^2\psi^1}{\partial x^2} = -\frac{D}{4\pi}\frac{\lambda A\sinh(\beta e\lambda\psi)}{1 + B\cosh(\beta e\lambda\psi)} \tag{26}$$

from Eq. (10), and

$$\psi^1 d\lambda = \frac{\partial}{\partial\lambda}(\lambda\psi^1)\,d\lambda - \lambda\frac{\partial\psi^1}{\partial\lambda}\,d\lambda \tag{27}$$

This then yields

$$\begin{aligned} G(l) = {} & -\frac{Da^2}{8\pi l}(\psi_0 - \psi_1)^2 - \int_0^l\int_0^1 \frac{DAa^2\sinh(\beta e\lambda\psi^1)}{4\pi[1 + B\cosh(\beta e\lambda\psi^1)]}\frac{\partial}{\partial\lambda}(\lambda\psi^1)\,d\lambda\,dx \\ & + \int_0^l\int_0^1 \frac{Da^2}{4\pi}\frac{\partial\psi^1}{\partial\lambda}\frac{\partial^2\psi^1}{\partial x^2}\,d\psi\,dx = -\frac{Da^2}{8\pi l}(\psi_0 - \psi_1)^2 + I_1 + I_2 \end{aligned} \tag{28}$$

On integrating I_1 with respect to λ we obtain

$$I_1 = -\int_0^l \frac{DAa^2}{4\pi e\beta B}\log_e\left[\frac{1 + B\cosh(\beta e\psi)}{1 + B}\right]dx \tag{29}$$

The second integral can be reduced by noting that

$$I_2 = -\frac{Da^2}{8\pi}\int_0^l\int_0^1 \frac{\partial}{\partial\lambda}\left(\frac{\partial\psi^1}{\partial x}\right)^2 d\lambda\,dx \tag{30}$$

which yields

$$I_2 = -\frac{Da^2}{8\pi}\int_0^l\left(\frac{\partial\psi}{\partial x}\right)^2 dx + \frac{D}{8\pi l}(\psi_0 - \psi_1)^2 \tag{31}$$

On substituting Eqs. (29) and (31) into Eq. (28) and changing the variable of integration from x to ψ, we obtain

$$G(l) = -\frac{Da^2}{8\pi}\int_{\psi_0}^{\psi_1} \frac{H + C\log\dfrac{(1 + B\cosh\beta e\psi)^2}{(1 + B)(1 + B\cosh\beta e\psi_0)}}{\left[H + C\log\dfrac{1 + B\cosh\beta e\psi}{1 + B\cosh\beta e\psi_0}\right]^{1/2}}\,d\psi \tag{32}$$

where

$$H = \left(\frac{\partial\psi(0)}{\partial x}\right)^2 \quad \text{and} \quad C = \frac{2a}{\beta eB}$$

Actually, what we wish to use in Eq. (24) is $G(x) - G(\infty)$, which latter is not zero. We calculate $G(\infty)$ as follows. From Eq. (11) we have

$$x(\psi') = \int_{\psi_0}^{\psi'} \frac{d\psi}{\left\{H + C\log\dfrac{1 + B\cosh\beta e\psi}{1 + B\cosh\beta e\psi_0}\right\}^{1/2}} \tag{33}$$

Now if $l \to \infty$, the denominator of the integrand must vanish as $\psi' \to 0$, which yields

$$H(\infty) = C\log\frac{1 + B\cosh\beta e\psi_0}{1 + B} \tag{34}$$

and then

$$G(\infty) = -\frac{Da^2}{8\pi}\int_{\psi_0}^{\psi_1} \frac{H(\infty) + C\log\dfrac{(1 + B\cos\beta e\psi)^2}{(1 + B)(1 + B\cos\beta e\psi_0)}}{\left[H(\infty) + C\log\dfrac{1 + B\cosh\beta e\psi}{1 + B\cosh\beta e\psi_0}\right]^{1/2}}\,d\psi \tag{35}$$

$G(x) - G(\infty)$ is then substituted for $G_{\text{elec}}(x)$ in Eq. (24).

We note in passing that a result essentially identical to Eq. (24) can be derived by applying statistical mechanical methods to a cell model. The calculation is similar to a somewhat simpler one we described earlier (*13*) and the method is illustrated in the next section of the present paper, so we omit it.

Use of Eq. (24) for the calculation of adsorption isotherms requires approximately 10 times as much computer time as is required by method one, Eq. (16). The shapes of the resulting isotherms are quite similar, as is seen by comparing Fig. 5 and those portions of the isotherms of Fig. 3 between 0 and 2×10^{-9} mole/cm^3, which correspond to the full horizontal

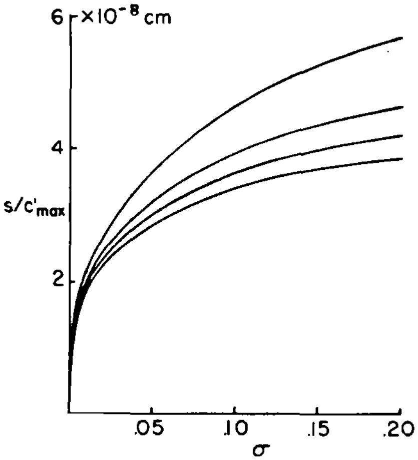

FIG. 5. Second method. Plot of surface excess of floc (s) versus floc concentration ($\sigma = c'/c'_{max}$); effect of c_∞. $\psi_0 = -100$, $\psi_1 = 100$ mv, $c_{max} = 10^{-3}$ mole/cm^3, $T = 300$°K, $a = 5 \times 10^{-8}$ cm. To compare Figs. 5 through 9 with 1 through 4, multiply both ordinates and abscissas by c'_{max}, which in most of the first four figures is 10^{-3} mole/cm^3.

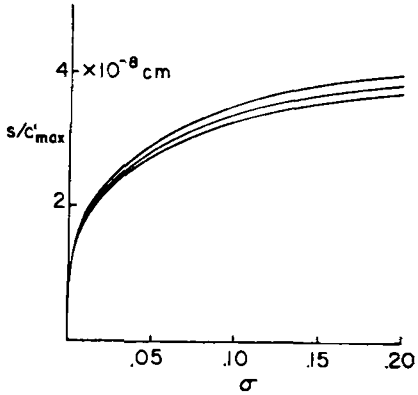

FIG. 6. Plot of s/c'_{max} versus σ; effect of c_{max}. $c_{max} = 5 \times 10^{-4}$, 10^{-3}, 2×10^{-3} mole/cm^3 from top down; $\psi_0 = -100$, $\psi_1 = 100$ mv, $c_\infty = 2 \times 10^{-4}$ mole/cm^3, $T = 300$°K, $a = 5 \times 10^{-8}$ cm.

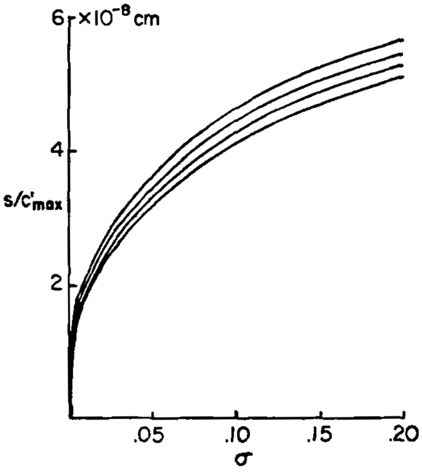

FIG. 7. Plot of s/c'_{max} versus σ; effect of temperature. $T = 300, 320, 340, 360$ °K from top down; $\psi_0 = -100$, $\psi_1 = 100$ mv, $c_\infty = 10^{-5}$, $c_{max} = 10^{-3}$ mole/cm^3, $a = 5 \times 10^{-8}$ cm.

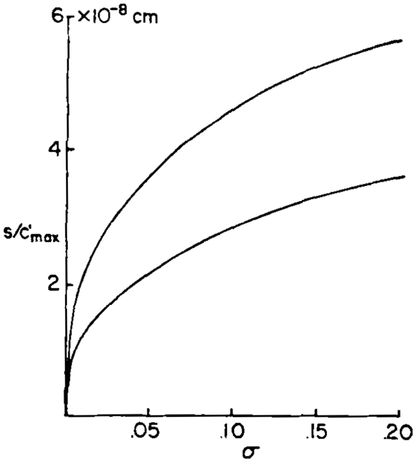

FIG. 8. Plot of s/c'_{max} versus σ; effect of ψ_0. $\psi_0 = -100, -50$ mv from top down; $c_\infty = 10^{-5}$, $c_{max} = 10^{-3}$ mole/cm^3, $T = 300$°K, $a = 5 \times 10^{-8}$ cm.

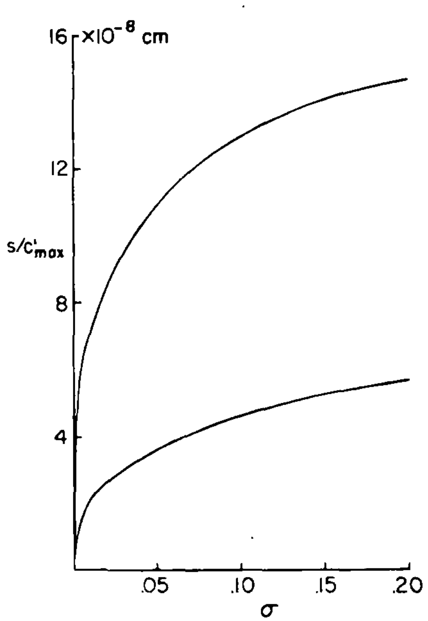

FIG. 9. Plot of s/c'_{max} versus σ; effect of a. $a = 10^{-7}$, 5×10^{-8} cm from top down, $\psi_0 = -100$, $\psi_1 = 100$ mv, $c_\infty = 10^{-5}$, $c_{max} = 10^{-3}$ mole/cm^3, $T = 300$°K.

scale of Fig. 5. Isotherms calculated by method two exhibit the expected decrease with increasing ionic strength (Fig. 5), and show a slight increase with increasing size of the ions composing the ionic atmosphere (Fig. 6). The temperature dependence of the isotherms is relatively slight, as shown in Fig. 7; a 60° temperature change results in a roughly 10% change in the isotherms. A decrease in the magnitude of the surface potential, ψ_0, of the surfactant layer decreases the adsorption isotherm, as shown in Fig. 8; an identical effect is observed if the zeta potential of the floc particles (ψ_1) is decreased. Increasing the size of the floc particles results in very marked increases in the adsorption isotherms, as seen in Fig. 9.

THIRD METHOD

Our second approach takes excluded volume effects of both the inert salt and the floc into account, and includes the effects of ionic atmospheres of both the surfactant-coated surface and the floc surface. It does not consider the screening of the electric potential produced by the surfactant-coated surface by other floc particles between this surface and the floc particle on which we are focusing our attention. It is difficult to estimate the extent to which such screening is effective; we examine here the limiting case in which it is completely effective. We note that we are still neglecting the mutual repulsions of the floc particles for each other. We use the grand partition function for a single site, and assume m cells (each capable of containing one floc particle) per site. We use Hill's notation (*18*).

The grand partition function for a single site is given by

$$\xi = \sum_{k=0}^{m} q(k)\lambda^k \tag{36}$$

$$q(0) = 1$$

$$q(1) = \sum_{i_1=1}^{m} \exp[-\beta E(i_1)]$$

$$q(k) = \sum_{i_1=1}^{m-k+1} \sum_{i_2=i_1+1}^{m-k+2} \cdots \sum_{i_{k-1}=i_{k-2}+1}^{m-1} \sum_{i_k=i_{k-1}+1}^{m} \exp[-\beta E(i_1)]$$

The summations over $i_2 \cdots i_k$ are readily shown to yield a factor

$$(m - i_1)!/(k - 1)!(m - i_1 - k + 1)!$$

so

$$q(k) = \sum_{y=1}^{m-k+1} \frac{(m - i_1)! \exp[-\beta E(i_1)]}{(k - 1)!\,(m - i_1 - k + 1)!}, \qquad m \geq k \geq 1 \tag{37}$$

This yields

$$\xi = 1 + \sum_{k=1}^{m} \sum_{i=1}^{m-k+1} \frac{(m - 1)!\lambda^k \exp[-\beta E(i)]}{(k - 1)!\,(m - i - k + 1)!} \tag{38}$$

Now from our earlier work (*12*), $\lambda = \sigma/(1 - \sigma)$, where σ is the density of floc particles per cell a large distance from the surface. Also, s, the average number of floc particles per site, is given by

$$s = \lambda\left(\frac{\partial \log_e \xi}{\partial \lambda}\right)_T$$

$$= \frac{\displaystyle\sum_{k=1}^{m} \sum_{i=1}^{m-k+1} \frac{k(m - i)!\,\lambda^k \exp[-\beta E(i)]}{(k - 1)!\,(m - i - k + 1)!}}{\displaystyle 1 + \sum_{k=1}^{m} \sum_{i=1}^{m-k+1} \frac{(m - i)!\,\lambda^k \exp[-\beta E(i)]}{(k - 1)!\,(m - i - k + 1)!}} \tag{39}$$

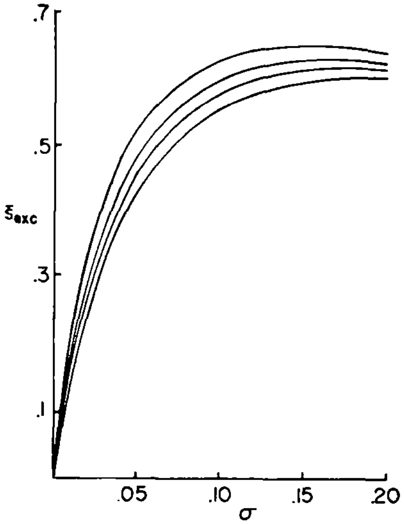

FIG. 10. Third model. Plot of $\bar{s}_{exc}$ versus σ; effect of c_∞. $c_\infty = 10^{-5}$, 5×10^{-5}, 10^{-4}, 2×10^{-4} mole/cm^3 from top down; $\psi_0 = -100$, $\psi_1 = 100$ mv, $T = 300$°K, $c_{max} = 10^{-3}$ mole/cm^3. If c'_{max} is taken as 10^{-3} mole/cm^3, then data from Figs. 10 through 14 should be multiplied by 1.184×10^{-10} (ordinates) and 10^{-3} (abscissas) for comparison with Figs. 1 through 4.

Then $s_{excess} = s - m\sigma$. In evaluating Eq. (39), we use the same formula for calculating the electrical energy of the floc particle nearest the surface as was used in the second method, $G(x_i) - G(\infty)$.

The third method requires roughly one-fifth as much computer time for the calculation of an isotherm as does the second method. Isotherms calculated by the third method show more linearity at low concentrations and rise to their maxima at lower concentrations than do isotherms calculated by the second method, as seen by comparing Figs. 5 and 10. The dependence of the isotherms on ionic strength is much less in Fig. 10 (third method) than in Fig. 5 (second method) as one goes to higher concentrations, as one would intuitively expect. The effects of the volume of the ions composing the ionic atmosphere (Fig. 11) are very similar to those observed for the second method (Fig. 6). The effects of temperature are also very similar for the two methods of approach as seen on comparing Fig. 12 with Fig. 7.

Figure 13 exhibits the expected increase in adsorption isotherm with increase in magnitude of the surface potential of the surfactant film, ψ_0.

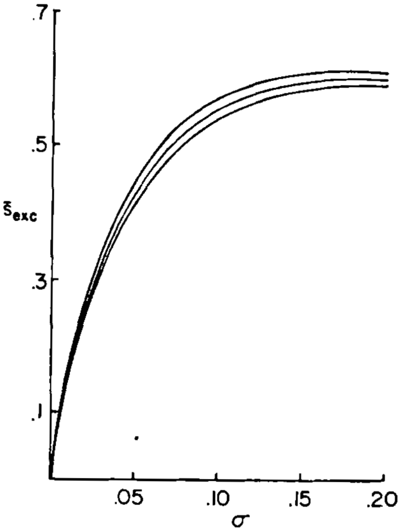

FIG. 11. Plot of $\bar{s}_{exc}$ versus σ; effect of c_{max}. $c_{max} = 5 \times 10^{-4}$, 10^{-3}, 2×10^{-3} mole/cm^3 from top down; $\psi_0 = -100$, $\psi_1 = 100$ mv, $c_\infty = 2 \times 10^{-4}$ mole/cm^3, $T = 300$°K, $a = 5 \times 10^{-8}$ cm.

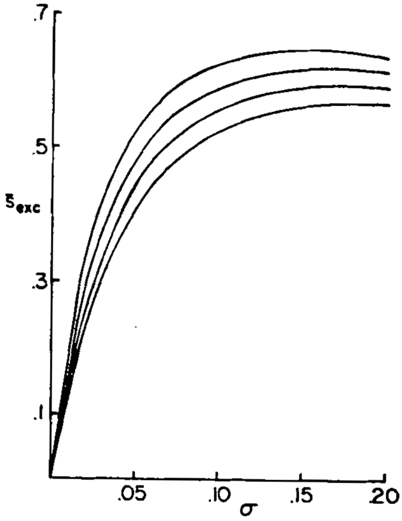

FIG. 12. Plot of $\bar{s}_{exc}$ versus σ; effect of temperature. $T = 300$, 320, 340, 360°K from top down; $\psi_0 = -100$, $\psi_1 = 100$ mv, $c_\infty = 10^{-5}$, $c_{max} = 10^{-3}$ mole/cm^3, $a = 5 \times 10^{-8}$ cm.

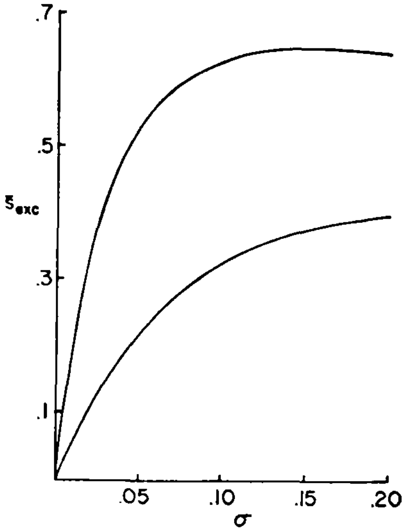

FIG. 13. Plot of $\bar{s}_{exc}$ versus σ; effect of ψ_0. $\psi_0 = -100$, -50 mv from top down; $\psi_1 = 100$ mv, $c_\infty = 10^{-5}$, $c_{max} = 10^{-3}$ mole/cm^3, $T = 300$°K, $a = 5 \times 10^{-8}$ cm.

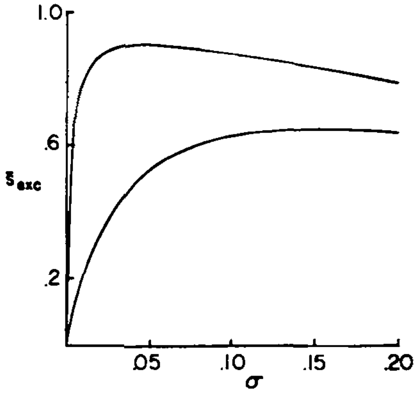

FIG. 14. Plot of $\bar{s}_{exc}$ versus σ; effect of a. $a = 10^{-7}$, 5×10^{-8} cm; $\psi_0 = -100$, $\psi_1 = 100$ mv, $c_\infty = 10^{-5}$, $c_{max} = 10^{-3}$ mole/cm^3, $T = 300$°K.

A comparison of the lower curves in Figs. 13 and 8 shows quite clearly the difference in behavior at low concentrations. This may be due, at least in part, to the fact that the third method involves the use of a discrete cell model, while the second does not. Figure 14 shows the very great differences which result as the size of the particles is increased. The behavior seen here is markedly different from that observed for the second method (Fig. 9). In either case, however, it is evident that anything which results in larger floc particle size *without* a corresponding decrease in floc particle zeta potential will improve the effectiveness of floc foam flotation separations.

CONCLUSIONS

We draw the following conclusions:

(1) Practically any reasonable model for floc adsorption on an ionic surfactant film predicts decreasing isotherms with increasing ionic strength and temperature, although the temperature dependence is weak.

(2) For ions of realistic size, the effect of the size of the ions constituting the ionic atmospheres of the floc particles and the surfactant film is rather small for all our models.

(3) Increasing the magnitude of the film surface potential or the magnitude of the floc charge (or zeta potential) increases the isotherms for all our models.

(4) Increasing floc particle size at constant zeta potential (or particle charge) increases the isotherms for all our models.

REFERENCES

1. R. Lemlich, in *Recent Developments in Separation Science*, Vol. 1 (N. N. Li, ed.), CRC Press, Cleveland, Ohio, 1972.

2. R. Lemlich (ed.), *Adsorptive Bubble Separation Techniques*, Academic, New York, 1972.

3. P. Somasundaran, *Separ. Purif. Methods*, *1*, 1 (1972).

4. P. Somasundaran, *Separ. Sci.*, *10*, 93 (1975).

5. D. J. Wilson, "Removal of Heavy Metals and Fluoride from Wastewaters by Foam Flotation Techniques," To Be Published.

6. S.-D. Huang and D. J. Wilson, *Separ. Sci.*, *11*(3), 215 (1976).

7. B. B. Ferguson, C. Hinkle, and D. J. Wilson, *Ibid.*, *9*, 125 (1974).

8. A. N. Clarke and D. J. Wilson, *Ibid.*, *10* (4), 417 (1975).

9. I. Sheiham and T. A. Pinfold, *J. Appl. Chem.*, *18*, 217 (1968).

10. J. W. Wilson and D. J. Wilson, *Separ. Sci.*, *9*, 381 (1974).

11. S.-D. Huang and D. J. Wilson, *Ibid.*, *10*, 405 (1975).
12. J. W. Wilson and D. J. Wilson, *Ibid.*, *11*(1), 89 (1976).
13. J. W. Wilson, D. J. Wilson, and J. H. Clarke, *Ibid.*, *11*(3), 223 (1976).
14. E. J. W. Verwey and J. Th. G. Overbeek, *Theory of the Stability of Lyophobic Colloids*, Elsevier, Amsterdam, 1948.
15. O. F. Devereux and P. L. deBruyn, *Interaction of Plane Parallel Double Layers*, M.I.T. Press, Cambridge, Massachusetts, 1963.
16. J. Jorné and E. Rubin, *Separ. Sci.*, *4*, 313 (1969).
17. J. R. Macdonald and M. K. Brachman, *J. Chem. Phys.*, *22*, 1314 (1954).
18. T. L. Hill, *An Introduction to Statistical Thermodynamics*, Addison-Wesley, Reading, Massachusetts, 1960, p. 130.

Received by editor January 13, 1976